

A Novel Systems Engineering Approach to the Design of a Precision Radial Velocity Spectrograph - the GMT-Consortium Large Earth Finder (G-CLEF)

William Podgorski^a, Jacob Bean^d, Henry Bergner^a, Moo-Young Chun^e, Jeffrey Crane^b, Ian Evans^a, Janet Evans^a, Gabor Furesz^a, Dani Guzman^c, Kang-Min Kim^e, Kenneth McCracken^a, Mark Mueller^a, Timothy Norton^a, Chan Park^e, Sang Park^a, David Plummer^a, Andrew Szentgyorgyi^a, Alan Uomoto^b, In-SooYuk^e

^a Harvard-Smithsonian Center for Astrophysics, 60 Garden St., Cambridge, MA 02140; ^bThe Observatories of the Carnegie Institution for Science, 813 Santa Barbara St., Pasadena, CA 91101; ^cPontificia Universidad Catolica de Chile, Vicuna Mackenna 4860, Macul, Santiago, Chile; ^d University of Chicago, 640 S. Ellis Ave, Chicago, IL 60637; ^e Korea Astronomy and Space Science Institute (KASI) 776, Daedeokdae-ro, Yuseong-gu, Daejeon, Republic of Korea

ABSTRACT

One of the first light instruments for the Giant Magellan Telescope¹ (GMT) will be the GMT-Consortium Large Earth Finder (G-CLEF). It is an optical band echelle spectrograph that is fiber fed to enable high stability. One of the key capabilities of G-CLEF will be its extremely precise radial velocity (PRV) measurement capability. The RV precision goal is 10 cm/sec, which is expected to be achieved with advanced calibration methods and the use of the GMT adaptive optics system. G-CLEF, as part of the GMT suite of instruments, is being designed within GMT's automated requirements management system. This includes requirements flow down, traceability, error budgeting, and systems compliance. Error budgeting is being employed extensively to help manage G-CLEF technical requirements and ensure that the top level requirements are met efficiently. In this paper we discuss the G-CLEF error budgeting process, concentrating on the PRV precision and instrument throughput budgets. The PRV error budgeting process is covered in detail, as we are taking a detailed systems error budgeting approach to the PRV requirement. This has proven particularly challenging, as the precise measurement of radial velocity is a complex process, with error sources that are difficult to model and a complex calibration process that is integral to the RV measurement. The PRV budget combines traditional modeling and analysis techniques, where applicable, with semi-empirical techniques, as necessary. Extrapolation from existing PRV instruments is also used in the budgeting process.

Keywords: echelle spectrograph, exoplanet, precision radial velocity, G-CLEF, GMT, error budget, systems engineering

1. INTRODUCTION

The GMT is a 25-meter, next-generation, optical/infrared telescope being developed for the purpose of conducting forefront scientific research in a broad cross-section of astrophysical topics. The telescope is designed around a segmented primary mirror composed of seven 8.4 m diameter circular mirrors and will have a collecting area nearly an order of magnitude larger than the largest single apertures in operation today. The aplanatic Gregorian optical design results in a fast telescope with a relatively wide field of view (20' diameter), when configured with a refractive field corrector, and a plate scale of 1"/mm at the final f/8 focus. Adaptive optics will be integral to the telescope through the use of deformable secondary mirrors with heritage in the MMT, LBT, VLT, and Magellan AO systems. With an angular resolving power of 10 milli arcseconds (mas) at 1 μ m, the GMT will image exoplanet systems, probe the environment around supermassive black holes, and explore distant galaxies on the scale of giant molecular clouds. The GMT will be located at Las Campanas Observatory in Chile, known for its excellent observing conditions.

The first light instrument for the GMT, G-CLEF, is being built by a consortium of institutions consisting of the Harvard-Smithsonian Center for Astrophysics, Carnegie Observatories, Pontificia Universidad Catolica de Chile, the Korean Astronomy and Space Science Institute, and the University of Chicago.

The G-CLEF spectrograph has been designed² to satisfy simultaneously the need for a general purpose high dispersion optical spectrograph, meeting the requirements for the GMT high resolution visible spectrograph (HRVS), and a

precision radial velocity spectrograph (PRVS). G-CLEF is designed to be a powerful instrument for a broad range of investigations in stellar astrophysics, cosmology, and astrophysics in general. A science goal for G-CLEF is measuring the mass of an earth-sized exoplanet orbiting a solar-type star in that star's habitable zone.

G-CLEF is an optical-band, fiber fed echelle spectrograph². The spectrograph optical design³ is shown in Figure 1. It is cross-dispersed and has a working pass band of 350 nm – 1000 nm. G-CLEF has been optimized to have extreme precision radial velocity (PRV) capability. For this reason it is vacuum enclosed⁴ and will be operated at a gravity invariant location on the GMT. The spectrograph is an asymmetric white pupil design and has a 300 mm diameter beam that is reduced to 200 mm post-dispersion. We are currently in the preliminary design phase, with a Preliminary Design Review scheduled in March 2015. Science operations are planned to begin in 2020.

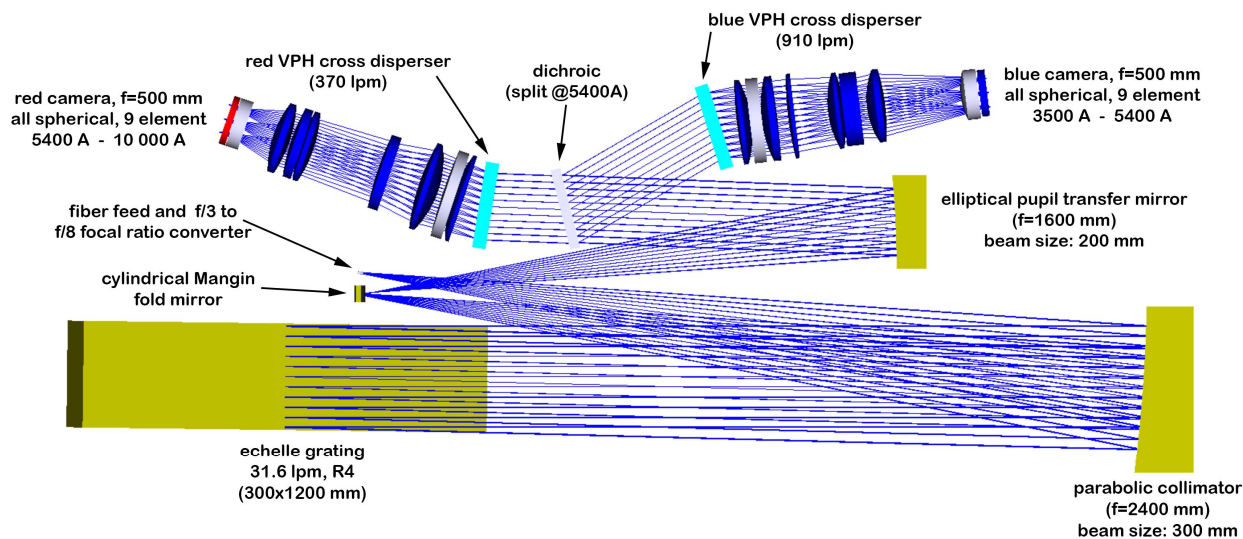


Figure 1 G-CLEF Spectrograph Optical Design

2. G-CLEF AND GMT SYSTEMS ENGINEERING AND REQUIREMENTS MANAGEMENT APPROACH

The GMT is being developed within a systems engineering framework that includes requirements flow down, traceability, error budgeting, and systems compliance. This is a traditional approach that has been used successfully in large military and space programs and is now being adapted for a large ground based telescope program. A systems engineering approach is required because the scale of the program greatly exceeds that of the previous generation ground based telescopes. The requirements flow down structure is illustrated in Figure 2. At the top level (Level 0) are the overall GMT and G-CLEF scientific objectives, which become the science drivers for the GMT and G-CLEF. These are broad statements of the scientific questions that the GMT and G-CLEF will explore. At the next level down (Level 1), the Level 0 science drivers are quantified into science and operational requirements for the GMT and G-CLEF. The GMT overall system level requirements reside at Level 2, and the GMT major system (telescope, software, adaptive optics, instrumentation and operations) requirements are at Level 3. The GMT Level 3 Instrumentation requirements and the G-CLEF science requirements flow down into the Level 4 G-CLEF instrument design requirements. The Level 1 through Level 4 requirements are all managed within GMT's automated requirements management system, Cognition Cockpit™. This system helps manage requirements flow down, traceability, and compliance by tying "parent" requirements at upper levels to "child" requirements at lower levels. Cockpit™ also assists in the requirements compliance process by automating the generation of verification matrices and recording compliance.

2.1 G-CLEF Instrument Requirements

GMT instrumentation requirements and G-CLEF science requirements flow down into the G-CLEF Instrument System Design Requirements, which are defined at Level 4 in the GMT requirements management system. The resulting document is the G-CLEF system requirements specification, which captures the top level G-CLEF design requirements.

Table 1 provides a summary of the major requirements for G-CLEF. The requirements reflect the multiple uses of G-CLEF for both precise PRV measurements and for more general high resolution optical band spectroscopy. To meet the multiple science objectives, G-CLEF must have a broad pass band, high resolution, high throughput, and a precise radial velocity measurement capability. G-CLEF is required to support four different modes of operation, and must use two science cameras, one for the blue wavelengths and another for the red. The performance requirements are therefore specified as a function of mode, and the throughput as a function of both mode and wavelength.

G-CLEF requirements are met, in many cases, by design. For example, the instrument passband and resolution are determined primarily by the optical design of the spectrograph, the cameras and the fiber feed system. The optical design of the spectrograph places the dispersed echelle orders onto the blue and red camera systems such that the wavelength coverage is met. Since the camera images the end of the fiber that feeds light into the spectrograph, the spectrograph resolution is primarily a function of the size of the fiber feed, and secondarily a function of the imaging properties of the spectrograph and camera system. The point spread function (PSF) of the spectrograph optical system must be small when compared with the size of the smallest fiber. A smaller fiber yields higher spectral resolution, but at the same time captures less of the input light, resulting in lower throughput. As the fiber is made smaller, the fraction of the light captured decreases, and the throughput goes down. The G-CLEF spectrograph is therefore required to operate in different modes with different spectral resolution/throughput characteristics; a high throughput mode with lower resolution and a medium throughput mode with somewhat higher resolution.

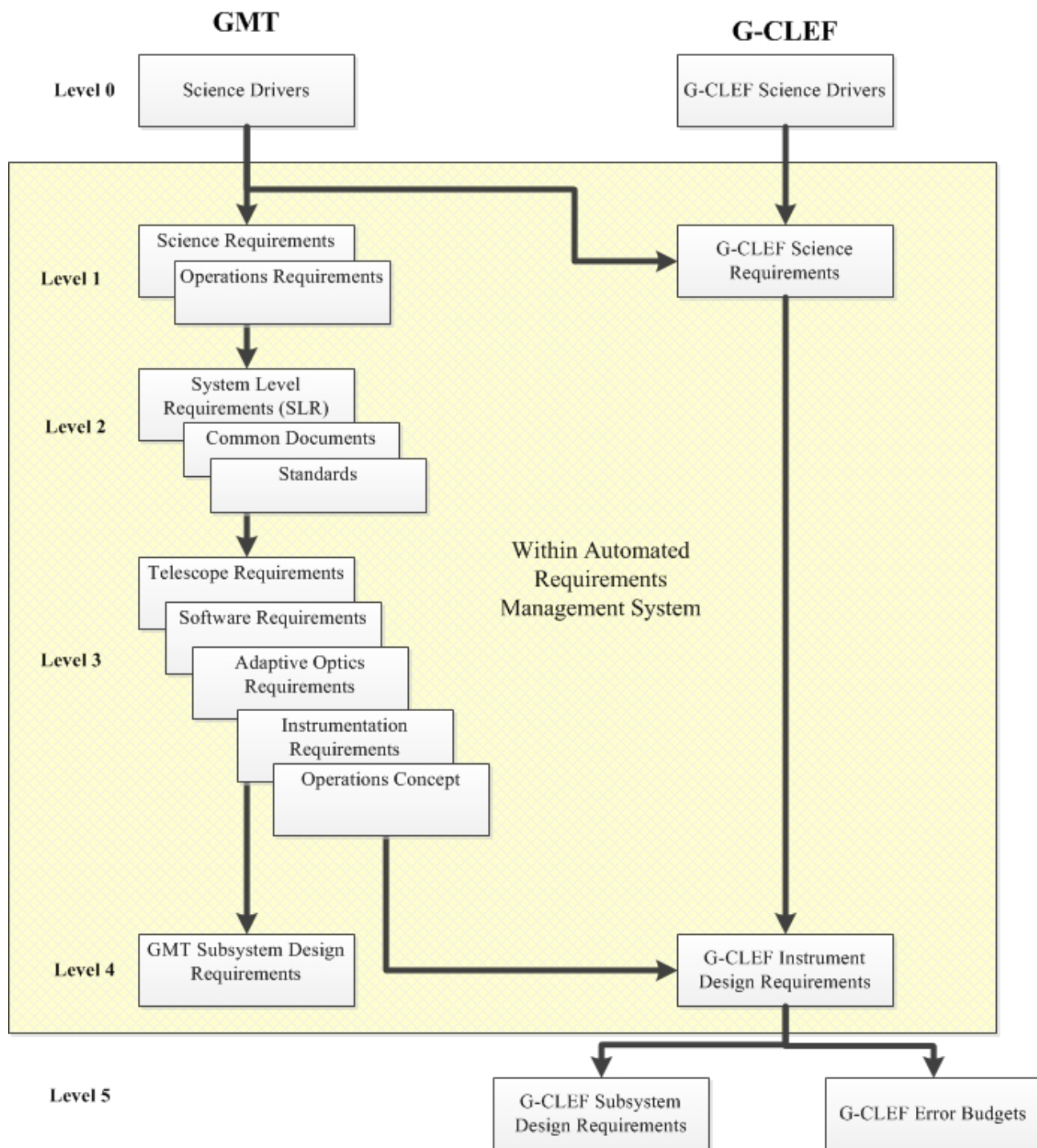


Figure 2 GMT and G-CLEF Requirements Structure and Flow Down

Table 1. Summary of Primary G-CLEF Instrument Requirements

Requirement Title	Requirement Statement					
Telescope Interface Conditions	Meet all requirements at GMT 75 th percentile seeing, with a FWHM of 0.79 arc seconds.					
Optical Feed	Provide an Optical Feed which deploys into the telescope beam and relays it into the G-CLEF fiber feed system.					
Wavefront Sensing	Provide an instrument wavefront sensing system which measures flexure induced telescope to instrument guide and focus offsets. Send these offsets to the GMT telescope control system for correction.					
Instrument Passband	350 nm to 1000 nm simultaneous wavelength coverage.					
Measurement Modes and Spectral Resolution	Scrambled Precision Radial Velocity mode (PRV) with spectral resolution > 100,000 (pupil sliced). High Throughput, non-scrambled PRV mode (PRV-NS) with spectral resolution > 100,000 (pupil sliced). High Throughput (HT) mode with spectral resolution > 20,000. Medium Throughput (MT) mode with Spectral Resolution > 35,000.					
Instrument Throughput		Wavelength(nm)	HT	MT	PRV	PRV-NS
		350	5.2%	3.2%	3.0%	3.4%
		500	12.7%	7.9%	7.5%	8.6%
		700	12.9%	8.0%	7.6%	8.7%
		800	12.0%	7.4%	7.1%	8.2%
		1000	1.9%	1.2%	1.1%	1.2%
Brightness Limit	Function with target brightness of M _R = 6 (or dimmer).					
Atmospheric Dispersion Compensation	Provide on-instrument atmospheric dispersion compensation.					
Operating Air Mass	Operate in all modes with air mass <= 2.					
PRV Single Measurement Precision	Be capable of making single PRV measurements with a radial velocity precision of 40–50 cm/s with a goal of 20 cm/s.					

The highest resolution specified for G-CLEF is 100,000 in the two PRV modes. The fiber size needed to achieve this resolution is small, on the order 100 μm in diameter. To achieve this resolution with reasonable throughput, the telescope image is pupil sliced, taking advantage of the GMT 7-element optical design. In this pupil sliced design the image is collimated and split up into 7 individual sub-pupils, coinciding with the GMT 7-element design. Each of the 7 sub-pupils are re-focused onto a small fiber. The 7 small fibers are then stacked at the spectrograph input in a direction normal to the dispersion direction. Use of the pupil slicer allows larger throughput than would otherwise be achievable with the small fiber size needed for spectral resolution of 100,000.

One final design feature which differentiates the two G-CLEF PRV modes is the use of an optical double scrambler to eliminate slit image variations for observations requiring the best possible wavelength scale stability, needed for the most precise PRV measurements. The double scrambler, however, introduces an approximate 15% throughput loss. G-CLEF therefore incorporates a non-scrambled PRV mode with the same resolution, providing more throughput but somewhat compromised wavelength stability.

2.2 G-CLEF Budgets

While many of the G-CLEF performance requirements can be met “by design”, others are much more complex and may be addressed by an error budget analysis. An error budget is typically used when a performance characteristic, for example the error in measurement of radial velocity, is subject to many different error sources that interact in complex ways. The error budget is simply an accounting tool that multiplies the sensitivity of the final result to each individual error source times an allocation for the error source and then sums (many times using a root sum squared method) these products to obtain a final error estimate. A variation of this is the throughput budget. In this case the individual throughputs of all elements that reduce the throughput of the system are multiplied together to yield the system throughput. The individual element throughputs may be varied (within limits) to achieve the required system throughput. A third form of budget is an observing efficiency budget. This is a timing budget in which the times for all actions needed to complete an instrument process, say preparation for and execution of G-CLEF observations, starting from a non-deployed state, are appropriately summed (some actions may take place in parallel with others) to yield the time needed for the activity.

The G-CLEF program makes use of various budgets to help manage development and the requirements compliance process. Four budgets have been developed; a PRV error budget, a throughput budget, an observing efficiency budget and spectrograph optical tolerance budget. The PRV error budget has been developed to help manage the PRV measurement precision requirement (40–50 cm/s). This is the most complex of the budgets and will be treated in detail in Section 3. Spectrograph throughput is key to meeting all of G-CLEF’s requirements and has a major impact on PRV measurement precision. The throughput budget is used to manage the spectrograph throughput requirements. This is treated in Section 4. The other two budgets are described briefly below.

Observing Efficiency Budget–The time needed to prepare for and execute observations is captured in this budget. It is important to optimize the operations of G-CLEF, since GMT time is precious. One aspect of this is to minimize the time needed to swap instruments. The sequencing of actions and the time needed for each action is captured in the budget. Parallel actions are factored in. This budget is compared to GMT specified state transition time requirements.

Spectrograph Optical Tolerance Budget–The effects of optical assembly and element manufacturing tolerances on the Spectrograph imaging quality are captured within this budget. The G-CLEF spectrograph optical system is composed of many different elements; several mirrors, the echelle and cross-dispersion gratings, a dichroic that splits the light into blue and red channels and multiple camera lenses for each channel. The spectrograph optical design produces an average RMS image diameter of about 7 μm in both the blue and red channels. We have a flow down requirement to maintain the RMS image diameter below 15 μm , which is one pixel on the detector, while the image of the smallest fiber entrance has a size much larger than this (85 μm or about 6 pixels). The tolerance budget uses sensitivities derived in ZEMAXTM and budgeted tolerances to meet this requirement.

3. PRV ERROR BUDGET

3.1 Precision Radial Velocity Requirements

A star with a planet will exhibit reflex motion in response to the planets gravitational pull. This leads to variations in the speed with which the star moves along the line of sight, i.e. the variations in the radial velocity of the star with respect to Earth. The radial velocity can be deduced from the displacement in the parent star's spectral lines due to the Doppler Effect. The radial-velocity method measures these variations in order to confirm the presence of the planet. A highly precise, or precision radial velocity, measurement is required to detect smaller Earth-type planets which are of interest.

G-CLEF requirements for PRV measurement precision (Table 1) have been set based on G-CLEF science requirements. Both the requirement (40–50 cm/s) and goal (20 cm/s) values represent advances over current PRV capabilities and are major scientific and engineering challenges. The requirement is interpreted as the one sigma value of a series of measurements over time, assuming that there are no target induced errors. Given the required instrumental precision, the measured PRV precision for an observation program on a suitable (low noise) target over a long enough time periods is expected to be 10 cm/s.

3.2 PRV Measurement Structure and Error Sources

The structure of radial velocity measurement error sources is shown in Figure 3. The two broad categories of errors are those which are instrumental and those which are related to the target itself. Target related error sources can introduce

errors with characteristic periods ranging from days to years. Stellar oscillations and granulation introduce errors with periods from a few minutes to a few days. The stellar surface can also contain dark regions (spots), and bright regions (plages), and occasional flares that may impact the RV measurement over periods ranging from a few days to a few months. Finally, stellar activity cycles may show effects with periods of years.

Even with a perfect instrument, target related errors (see Figure 3) must be mitigated by using a carefully developed long term observation program that averages the target errors to produce more accurate radial velocities. Instrumental errors add another degree of difficulty to the measurement process. Since measurements will be made over long periods of time, the instrument must provide high absolute accuracy over these time periods. In the short term an instrument can be made mechanically stable enough to provide highly precise radial velocity measurements, however, any instrument will drift over longer time periods, especially if the instrument configuration is varied, such as by a re-pressurization cycle or thermal upset. These effects must be calibrated out, hence the importance of having an extremely accurate calibration process, stable over long time periods. Since the PRV measurement precision depends on the target, instrument, and observation program, and the target error (noise) magnitudes vary widely, the PRV measurement precision requirement cannot be stated at the top most level. Instead, the requirement is stated at the instrument level, as shown in Figure 3.

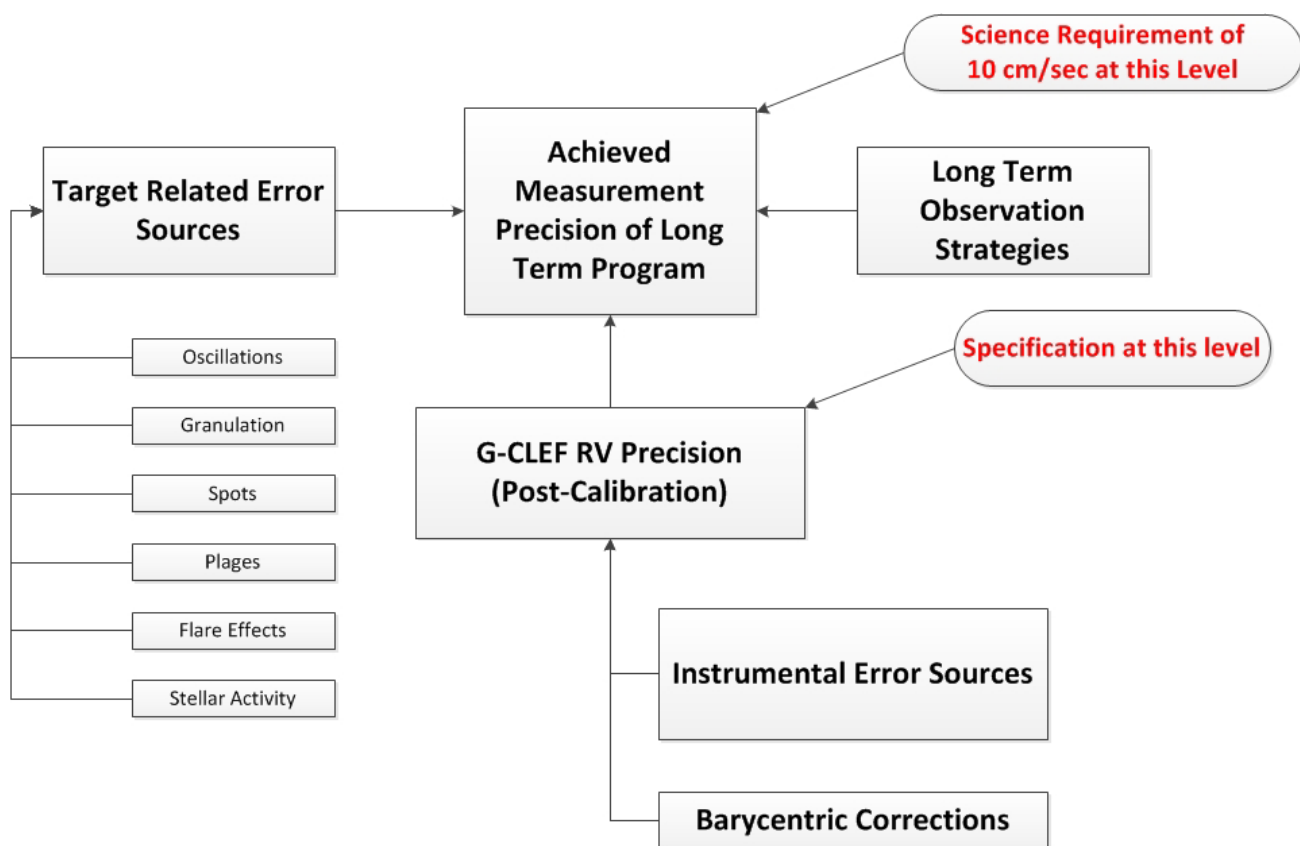


Figure 3 Radial Velocity Measurement Error Sources

3.3 PRV Budget

Development of a PRV error budget is a particularly challenging task. Some of the reasons for this are:

1. Many sensitivities not amenable to analysis, therefore the budgeting process must rely to some extent on extrapolations from current instruments;
2. Interaction of measurement and calibration is complex;
3. Some error sources not well understood, e.g., detector effects such as variable effective pixel size.

Although the working PRV error budget is kept in an Excel spreadsheet, the structure of the budget may be best illustrated graphically, as is shown in Figure 4. The G-CLEF instrument single measurement RV precision is specified at the top level of the budget.

PRV BUDGET STRUCTURE

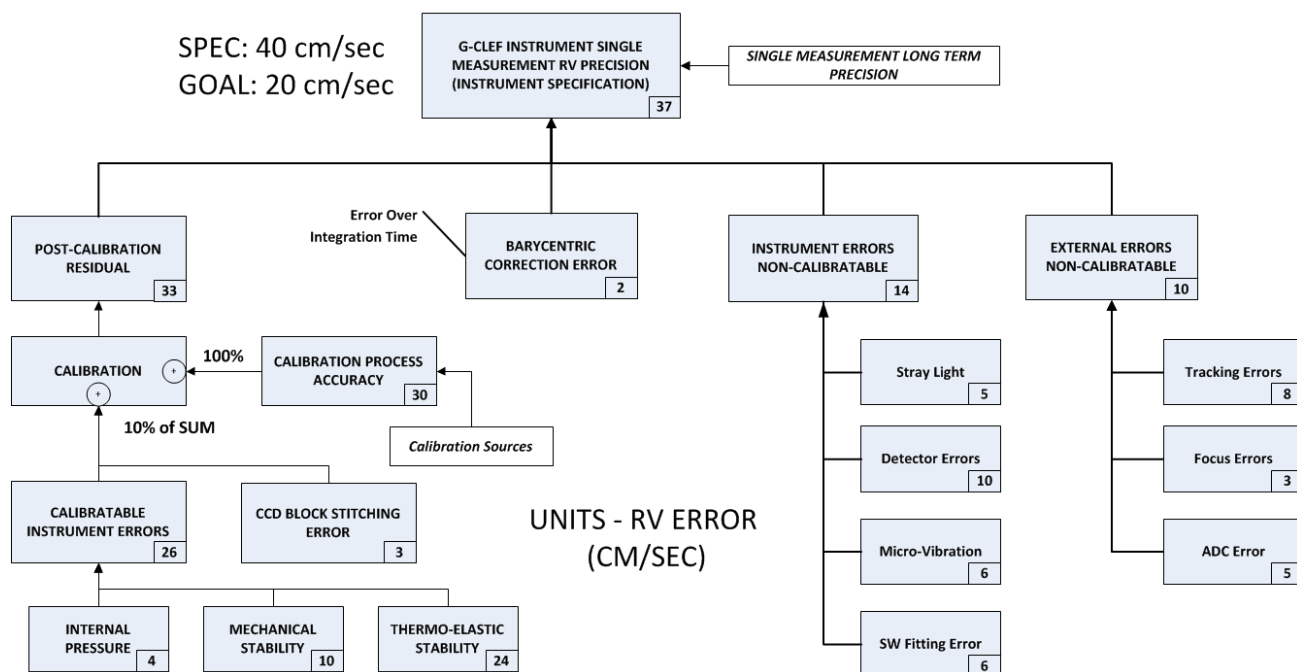


Figure 4. PRV Error Budget Top Level Structure

The top level budget estimate (37 cm/s) is an RSS roll-up of the following four terms:

1. Post-calibration residual (33 cm/s), including:
 - a. Calibration Process Accuracy;
 - b. Instrument Calibratable Errors;
2. Barycentric Correction Error (2 cm/s);
3. Instrument Errors, Non-calibratable (14 cm/s);
4. External Errors, Non-calibratable (10 cm/s).

Post-Calibration Residual

The “Post-Calibration Residual Error” term captures the residual error after the calibration has been applied to those errors which are amenable to calibration. The concept is to determine which of the error sources will apply to the calibration signal and which will not. Having this division, we then assume that the error remaining after the calibration is complete will be equal to the sum of a calibration accuracy term plus a fraction of the calibratable errors, in our case we assumed 10%, based on current practice. In the error budget, instrument errors are separated into calibratable and non-calibratable instrument errors. Examples of calibratable errors would be the effects of spectrograph internal pressure and the slowly varying thermo-elastic deformations of the spectrograph, each of which affects both the calibration and star light, and vary slowly enough that the calibration run sees essentially the same error (for expected measurement times). In summary, the residual error from the calibration process is modeled as a sum:

100% of the calibration process accuracy + 10% of calibratable instrument errors.

The “Calibration Process Accuracy” places an absolute floor on this error term. Additional errors are proportional to the magnitude of the error to be calibrated out, so it is important to make these errors as small as possible. The “Calibratable Instrument Errors” are shown in the roll-up below the Post-Calibration residual term.

Calibration Process Accuracy and Calibration Sources

The calibration process accuracy is a key error term in the budget because: 1) in an observation program we must utilize numerous measurements over a long time period, and 2) the stability of the instrument without calibration does not support the required accuracy over the time periods needed for an observation program. We must therefore rely on a robust, accurate calibration to tie the measurements together.

The baseline calibration source will be a state-of-the art thorium-argon⁵ hollow cathode lamp source similar to that used in the HARPS spectrograph. Using the latest calibration methods as developed for HARPS we expect to be able to achieve an accuracy of 30 cm/s. In order to achieve the G-CLEF goal, we must use other advanced calibration sources as well. Two advanced sources have been considered: 1) laser frequency comb and 2) ultra-stable white light etalon. We are actively working on these sources in collaboration with scientific partners^{6,7} and plan to carry out this work in parallel with the development of the baseline spectrograph with the ThAr calibrator. An allocation of 5 cm/s is made for the accuracy of the advanced calibration source.

Calibratable Instrument Errors

The calibratable instrument errors roll-up is shown in the budget. It includes the following sub-terms:

1. Internal Pressure Stability;
2. Spectrograph Mechanical Stability;
3. Optical bench moisture loss effects (if a composite bench is used);
4. Spectrograph Thermo-elastic Stability;
5. Block Stitching Error.

Internal Pressure Stability-This term is due to the fact that the G-CLEF spectrograph operates in a vacuum vessel, but with the vacuum pumps turned off during observations. The internal pressure thus will rise over time. The RV error arising from this source is due to the change in index of refraction as the pressure rises, according to the equation:

$$\text{where } \lambda(\text{air}) = \lambda(\text{vacuum}) / n, \\ \lambda = \text{wavelength, } n = \text{Index of refraction, and } \Delta RV = \Delta \lambda / \lambda(\text{vac})$$

The index change with pressure is calculated from the Edlen equation⁸. Based on vacuum simulations we expect that a pressure of 4.0×10^{-4} torr would be present after about 12 hours without pumping. This would lead to an RV error of 4 cm/s, which is incorporated into the error budget. This term is considered to be calibratable since the calibration light will pass through the same gas in the spectrograph as the source light and the change in pressure is slow relative to the measurement times.

Spectrograph Mechanical Stability-These errors arise from three sources: 1) the change in atmospheric pressure (external to the spectrograph) causing structural deformation of the spectrograph, resulting in lateral shifts of the spectra and focus errors, and 2) the motion of the G-CLEF spectrograph supporting structure (floor) as the telescope moves in azimuth, resulting in lateral shifts of the spectra and focus errors and 3) the instability of the materials in the spectrograph over the duration of a measurement, including the effects of moisture desorption from a composite bench. These error terms affect both calibration and star light, and are expected to be small and slowly varying compared to the measurement times, and are thus considered calibratable. An overall allocation of 10 cm/s has been made, split equally between external pressure and floor motion. These effects are amenable to analysis, which will be done in the preliminary design phase.

Spectrograph Thermo-elastic Stability - These errors arise from time varying temperatures in the spectrograph, both overall bulk temperature and temperature gradient. They cause thermo-elastic distortions of the spectrograph optical

system which in turn shifts the spectra on the detector and changes the focus. Both calibration and star light are affected, and the errors are slowly varying with respect to measurement times. They are considered calibratable. In the error budget we have made an allocation of 24 cm/s for this term, split equally between soak and gradient effects. We have performed preliminary analyses of these effects, using the concept design as a basis. The analyses (described below) show that we meet the allocation for soak error but exceed it for gradient error. Work to improve the performance in this area will be performed in the preliminary design phase.

A preliminary finite element analysis of thermo-elastic stability errors has been performed. The analysis used the concept design study spectrograph design. Thermal errors assumed were: 1) 0.001 C bulk temperature and 2) ± 0.001 C gradient in each axis, applied as separate cases. The thermal errors were applied as loads in the finite element analysis (FEA) model and resulting optical component motions were input to the SAO "Bisens" software, which computes image shifts in the focal plane (lateral in two axes and defocus). The largest error resulting from the analysis was 110 Å of lateral motion, which translates to 55 cm/s. RV error. We expect to lower this by using low CTE materials and improving thermal control.

Block Stitching Error-Another term in the Post-Calibration Residual error is the "CCD Block Stitching Error", which is a calibratable detector effect due to the fact that the lithographic process for making the CCD detectors steps the lithographic mask in discrete steps, creating a block of pixels in each step, and therefore is subject to block to block positional errors which must be "stitched" together in the wavelength solution, since the Doppler shift can move spectral features near the edge of a block to a different block. This error term has an allocation of 3 cm/s for both requirement and goal.

Barycentric Correction Error

Velocities due to the Earth orbiting the Sun and rotating around its axis have to be extracted from the radial velocity of the measured star. The observed radial velocity is corrected for the motion of the observer in the direction of the observation. One must calculate the intensity weighted midpoint of the exposure and use this as the time of the observation to calculate the barycentric correction value. To assure this G-CLEF will employ an exposure meter to accurately determine the true mid-point of the exposure, which can shift significantly due to changes in atmospheric conditions. The accuracy of this correction is expected to be in the few cm/s range, based on available prediction software and short integration times⁹. We have made an estimate of 2 cm/s for this error term.

Instrument Errors-Non-Calibratable

As shown in Figure 4, this error term includes four sources, some of which are hard to quantify, but which are expected to contribute errors that are not amenable to calibration.

Stray Light-A potential, but difficult to quantify, error source. The opto-mechanical design eliminates potential sources as much as possible via proper baffling. Ghost/scattered light analysis will be performed in the design phase. An error allocation of 5 cm/s. has been made.

Detector Errors-This term captures errors that are associated with the detector and detector readout, with an allocation of 10 cm/s. These errors have been the subject of active discussion, but are difficult to quantify in the PRV spectrograph. Some of the effects under consideration are non-identical pixels, CCD inhomogeneity, detector heating on readout, detector thermal control errors, and dependence of CTE on the amount of charge carried in the clocking

Micro-vibration-Even at the μg level, micro-vibration can cause errors in the measurement of PRV that cannot be calibrated out because they are not systematic. A vibration analysis of the concept design study optical bench was performed, using a 1 μg input. This input level is considered to be achievable with proper isolation. The resulting motion of the detector is 100 Å, which in the worst case would give a 5 cm/s RV error. This value is carried in the budget. However, we believe that this is a very conservative allocation, because the effect of vibration is to broaden the lines, not shift them. This broadening give a smaller error than a shift of the same magnitude, but the analysis has not yet been performed.

Software Fitting Error-Fitting of the wavelength solution to the data can have numerical errors which must be accounted for. We have allocated 6 cm/s RV error for this term.

External Errors, Non-Calibratable

These errors are the result of the spatial variability of the light entering the fiber. Much of this variability is smoothed out by scrambling within the fiber¹⁰, but the residual variability moves the line positions within the spectrograph during the observation, causing RV errors. These effects are due to external factors that are not present during calibration, and so are non-calibratable. Three external sources of error are included within this term: 1) tracking errors 2) focus errors, and 3) imperfect and variable atmospheric correction errors. The tracking and focus error terms each have two sub-components: 1) telescope errors, and 2) errors between the instrument and telescope, caused by flexure, and imperfectly corrected by the on-instrument wavefront sensing capability.

Guiding Errors-The two sources of tracking error are telescope error, estimated to be 68 mas RMS radius error and on-instrument tracking correction error, allocated as 10 mas RMS radius error. Combined, the errors equal 69 mas. The impact of guiding errors on RV accuracy has been assessed by applying results from reference 11. The results from the reference indicate that, for image displacements less than $\frac{1}{4}$ of the fiber diameter, the RV errors are negligible. This result depends on having a scrambling gain of 10,000, obtained using octagonal fibers and an optical double scrambler. The G-CLEF PRV aperture diameter is 800 mas, so the RMS error from telescope tracking is much less than $\frac{1}{4}$ of the diameter. Even though the data would indicate that the RV error would be negligible, we have made a conservative allocation of 8 cm/s for guiding error term in the requirement budget.

Focus Errors - Focus errors can also lead to RV errors by the mechanism of degrading the image quality input into the fiber system. This is expected to be a small, if not negligible, error term, since it is changing the fiber feed in a symmetrical manner, but the sensitivity has not yet been analyzed. Two sources of focus error are considered, those from the Telescope and those from the on-instrument focus sensor that provides data for correction of instrument to telescope focus errors. An allocation of 3 cm/s has been made for this term.

ADC Errors-The G-CLEF Atmospheric Dispersion Compensator (ADC) is used to color correct for atmospheric dispersion of the image. The dispersion of the colors in the image will have a small impact on the RV accuracy. The specification for ADC error is 0.2" (PV) at maximum zenith distance. The impact of ADC errors on RV error is expected to be small, but it is a somewhat more complex error term due to its wavelength dependence and as yet we have not done the sensitivity analysis. We have therefore made an allocation of 5 cm/s for this term in the requirement and goal budgets.

PRV Budget Summary

A preliminary error budget for radial velocity measurement error has been developed. The budget relies heavily on current experience. Analysis is used, where applicable. Error terms have been quantified. The calibration process has been addressed using a semi-empirical method. G-CLEF expects to meet its ambitious requirements using a broad passband, high throughput (result of GMT area), high resolution, pupil sliced spectrograph design. A near-zero CTE composite optical bench is also under consideration. We plan to meet our PRV measurement goals by incorporating advanced, ultra-stable calibration sources such as the laser comb, and by taking advantage of the higher throughput and stability which will be available when the GMT adaption optics (AO) capability becomes available.

4. THROUGHPUT BUDGET

A throughput budget has been developed to help manage the G-CLEF throughput requirement. Throughputs of all of the elements within G-CLEF have been estimated based on the best information available at this time. They are a function of wavelength and, in some cases, observing mode. The throughputs are entered into an EXCEL spreadsheet and multiplied together to yield the overall instrument throughput. The throughput budget structure is shown in Figure 5. G-CLEF throughput is the product of the throughputs of three sub-systems:

1. Front End;
2. Fiber System;
3. Spectrograph.

The structure of each of the G-CLEF subsystems is also shown in Figure 5.

Front End Subsystem

The Front End Subsystem optical layout is shown in Figure 6. The function of the front end is to extend into the GMT beam and pick-off a 1.5 arc minute field of view and relay it to the slit apertures, which feed the fiber system. The front end contains the tertiary mirror, a collimating triplet, two atmospheric dispersion compensation prism assemblies and a focusing triplet. The front end also includes a guide camera and focus sensor, which is not shown since it does not impact G-CLEF throughput. The tertiary mirror will be coated with a multi-layer dielectric coating which should have reflectance > 98% across the band. The front end lenses will have high internal transmission and will be AR coated to minimize reflective losses. Throughput data on candidate coatings and current baseline glasses has been used in the throughput spreadsheet to calculate front end throughput.

Fiber Subsystem

The fiber system includes the optical fibers and associated components which relay the light from the slit aperture into the spectrograph. The items which are included in the fiber system throughput are shown in Figure 5. The first element in the fiber system is the slit aperture. The slit aperture is located at the relayed telescope focus (Figure 6). There is a separate aperture for each of the four observing modes. Each of the two PRV modes uses a separate 800 μm diameter circular aperture (0.800" given the GMT nominal plate scale of 1 mm/"). In the HT and MT modes the fiber ends are placed in the slit plane. The four apertures are located on a slit plate assembly that translates relative to the relayed telescope beam to bring the desired aperture into the beam.

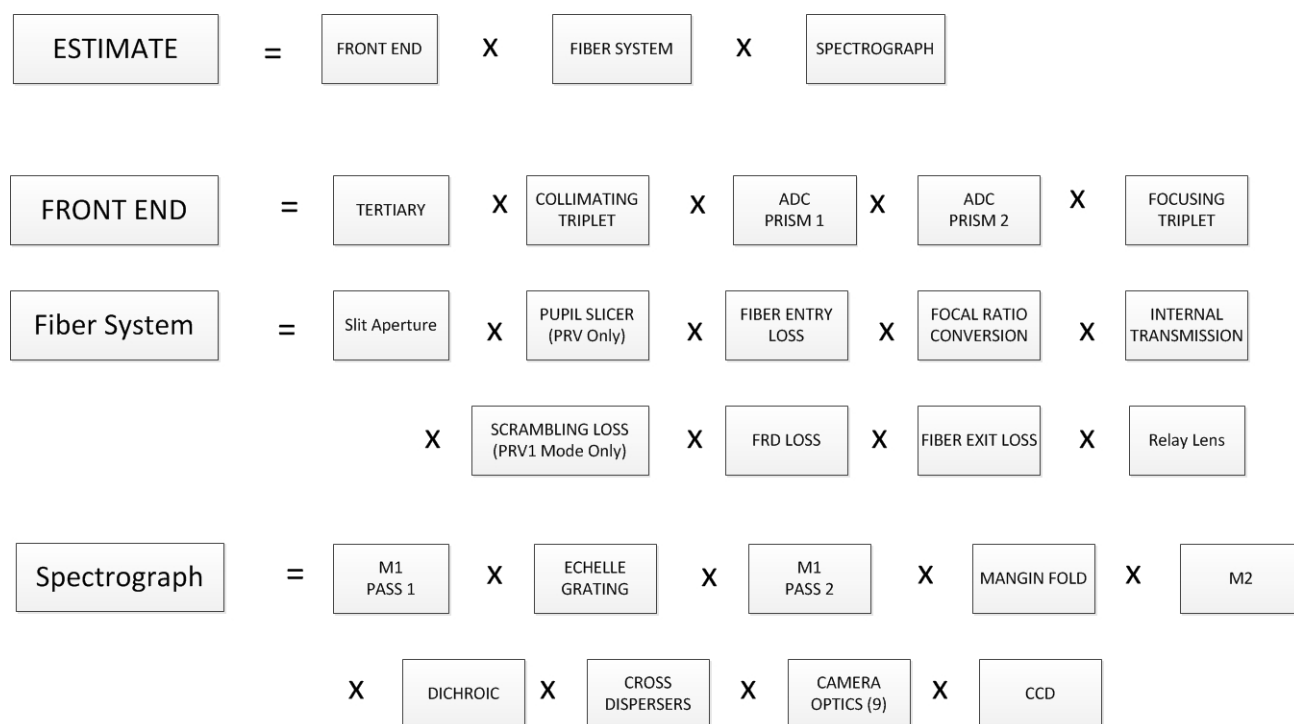


Figure 5 Throughput Budget Structure

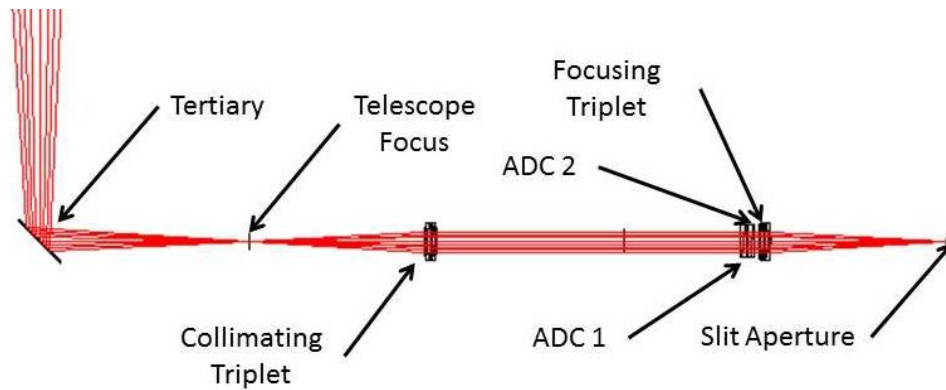


Figure 6. Optical Layout of the G-CLEF Front End Assembly

The slit aperture throughput is a function of the aperture size and the telescope PSF. Since G-CLEF will initially operate in the GMT natural seeing mode, without the benefit of adaptive optics, we have calculated the throughput using the Natural Seeing mode PSF (estimate provided by the GMT Organization), which is dominated by atmospheric turbulence effects. The Full Width at Half Maximum (FWHM) for the 75th percentile natural seeing is estimated to be 0.79". The atmospheric turbulence dominated PSF has been modeled as a two dimensional Gaussian or, alternatively, as a Moffat Function¹². A summary of the slit aperture throughput is given in Table 2.

Table 2 - Slit Aperture Throughput

Observing Mode	Aperture	Gaussian Throughput	Moffat Throughput
PRV, PRV-NS	800 μm (.8") circular	50.7%	37.9%
HT	1200 μm (1.2") Octagonal	81.4%	62.6%
MT	800 μm (.8") Octagonal	52.6%	39.3%

As discussed above, pupil slicing optics are used in the two PRV modes. The pupil slicers each consist of a collimating lens and a 7-element focusing lens array. Throughput of the pupil slicer elements is accounted for only in the PRV modes.

The telescope beam enters the fiber after passing through the pupil slicer (PRV modes) or directly into the fiber at the slit plane. Reflection losses at fiber entry (and later on at exit) are minimized by the use of AR coatings on polished (or cleaved) ends.

Focal Ratio Degradation and Management-After the input beam enters the fiber at the telescope focal ratio of f/8 the fiber is down-tapered to an internal f/3 focal ratio, incurring a focal ratio conversion loss. The f/3 focal ratio is preserved until the fiber is terminated at a polished end (within the spectrograph vacuum chamber). The beam then enters a small relay lens which converts the exiting f/3 beam to the f/8 beam needed to feed the spectrograph. There are losses at the fiber exit, mitigated by an AR coating, and losses in the focal ratio conversion (relay) lens. This focal ratio management technique minimizes focal ratio degradation (FRD) losses within the system. The two focal ratio conversion losses plus the residual FRD losses, when combined, are much less than the FRD losses which would result if focal ratio conversion were not done.

Two other loss terms are present in the fiber system: internal transmission losses, which are a function of wavelength, and losses in the optical double scrambler, which is used only in the scrambled PRV mode. A Polymicro FBP low OH content fiber is used because of its good blue response and lack of an OH absorption feature in the red. The length of the science fiber run is 15 m. The internal transmission for this 15 m run is plotted in Figure 7.

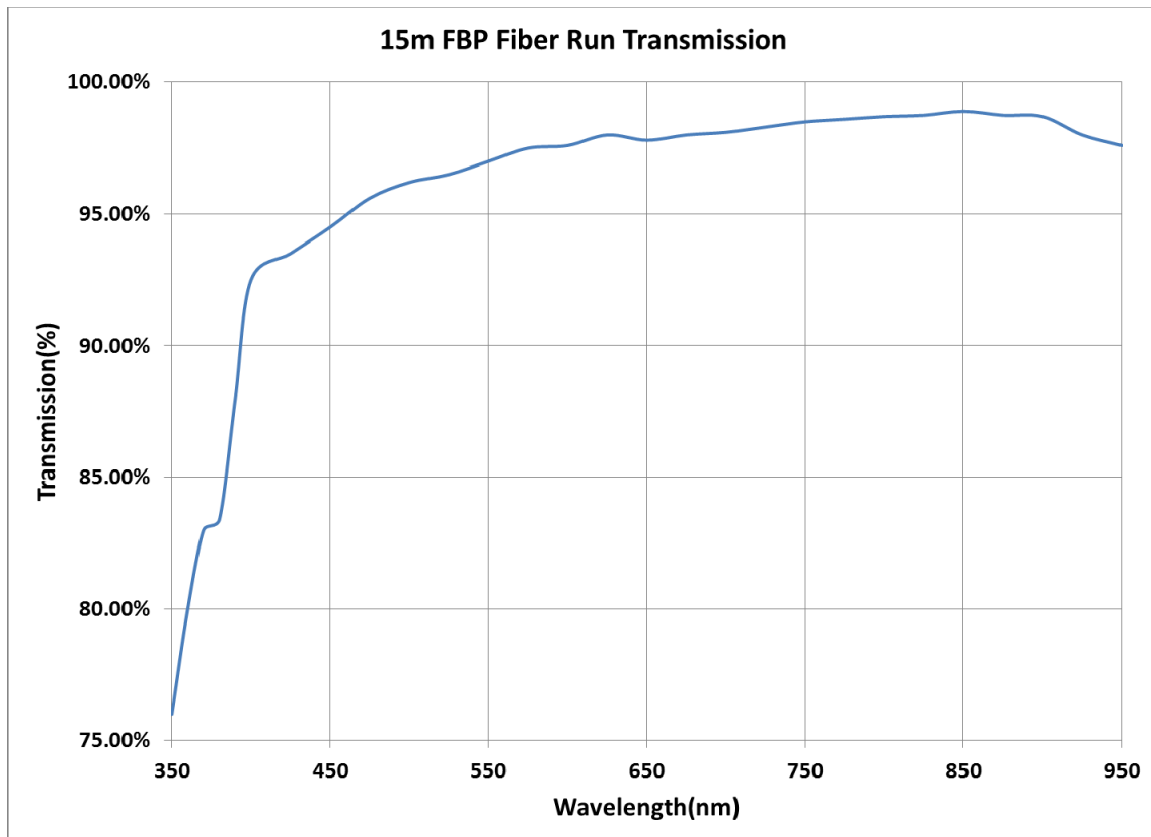


Figure 7. Internal Transmission Loss for 15 m Fiber Run

Spectrograph Subsystem

The spectrograph optical layout is shown in Figure 1. The f/8 beam exits from the focal ratio converter and follows the following optical path:

1. Reflects off an off-axis parabolic collimator (M1 Pass 1);
2. Reflected and dispersed from the echelle grating (echelle);
3. Reflected (2nd pass) off the off-axis parabolic collimator (M1 pass 2) and focused;
4. Reflected off a cylindrical Mangin fold mirror;
5. Reflected and collimated off an elliptical transfer mirror (M2);
6. Red wavelengths are transmitted, blue reflected by a dichroic into separate blue and red camera systems;
7. Each band passes through separate blue or red cross-dispersers;
8. Each band passes separately through a 9 lens camera (blue or red);
9. Each band is imaged by a CCD (blue or red).

The throughput of each element has been estimated using data from potential vendors of the individual components. High reflectance multi-layer dielectric coatings are assumed for the mirrors. The grating reflectance is based on similar gratings produced by Richardson. All of the camera lenses are optimized for their band pass and have AR coatings. The baseline detector is an E2V CCD231-C6 BI sensor (6144 x 6160, 15 μm pixels). The blue and red detectors will be optimized for their individual band passes. Quantum efficiency data from E2V has been used in the budget estimate.

Throughput Budget Estimates

A portion of the throughput budget spreadsheet is shown in **Table 3**. The observing mode (PRV1 MODE, PRV-NS MODE, HT MODE, and MT MODE) and seeing condition (GAUSS-75%, GAUSS-50%, GAUSS-25%, MOFFAT-

75%, MOFFAT-50%, and MOFFAT-25%) are selected using drop-down lists. Throughputs for the three major subsystems are calculated from the individual sub-components (the front end subsystem is shown in the figure). Throughput for these subsystems is multiplied to yield the G-CLEF overall estimate, which is compared to the G-CLEF requirement to yield a margin. The G-CLEF estimate is also multiplied by the GMT telescope throughput to give a (G-CLEF + telescope) estimate.

Current estimates for the four modes are shown in Figure 8. The curves show a discontinuity at ~540 Å, which is the cross-over between the blue and the red camera systems.

The throughput budget spreadsheet has been designed to be a working tool which is easily revised as new data is generated. The budget will be kept throughout the program and updated as required. Our starting point has been data generated in the concept design phase. We have made revisions as the design has evolved in the preliminary design phase. The cameras and fiber system have already been revised based on this ongoing work. As we move towards Critical Design Review the estimates will be refined, particularly as we receive vendor proposal for sub-components. During the build phase the data will be updated with measured information and the “Estimate” will evolve into an “As-Built” throughput calculation.

Table 3. G-CLEF Throughput Budget (Upper Section)

G-CLEF Throughput Budget																					
Is PRV Mode?	MODE =				PRV1 MODE				SEEING =				GAUSS-75%								
TRUE																					
Element	Blue Camera								Red Camera												
	Wavelength(nm)								Wavelength(nm)												NOTES
	350	375	400	425	450	500	538	539	550	600	650	700	750	800	850	900	950	975	1000		
G-CLEF + Telescope																					
PRV1 MODE	0.028	0.046	0.064	0.079	0.074	0.074	0.057	0.040	0.042	0.058	0.064	0.070	0.068	0.060	0.053	0.037	0.023	0.016	0.009		
Telescope Overall	0.711	0.711	0.711	0.711	0.711	0.711	0.682	0.682	0.669	0.669	0.669	0.669	0.619	0.619	0.619	0.619	0.619	0.619	0.619		
Telescope M1	0.843	0.843	0.843	0.843	0.843	0.843	0.826	0.826	0.818	0.818	0.818	0.818	0.787	0.787	0.787	0.787	0.787	0.787	0.787	SLR Table 5 (Minimum Spec)	
Telescope M2	0.843	0.843	0.843	0.843	0.843	0.843	0.826	0.826	0.818	0.818	0.818	0.818	0.787	0.787	0.787	0.787	0.787	0.787	0.787	SLR Table 5 (Minimum Spec)	
G-CLEF REQUIREMENT																					
PRV1 MODE	0.031	0.045	0.066	0.081	0.076	0.075	0.060	0.042	0.046	0.062	0.070	0.076	0.079	0.071	0.062	0.043	0.027	0.019	0.011		
MARGIN																					
PRV1 MODE	26.1%	42.6%	37.6%	37.5%	37.3%	38.3%	38.0%	38.3%	37.8%	37.6%	37.6%	37.4%	37.6%	37.7%	37.5%	37.1%	34.9%	36.4%	33.0%		
G-CLEF Overall ESTIMATE																				Front End + Fibers + Spectrograph	
PRV1 MODE	0.039	0.064	0.090	0.111	0.105	0.104	0.083	0.059	0.063	0.086	0.096	0.104	0.109	0.097	0.085	0.060	0.037	0.026	0.015		
G-CLEF Front End (Relay/ADC)	0.887	0.901	0.887	0.893	0.871	0.885	0.868	0.868	0.860	0.867	0.860	0.869	0.881	0.869	0.867	0.857	0.859	0.861	0.871		
G-CLEF Tertiary Mirror	1.000	1.000	1.000	0.999	0.998	0.990	0.987	0.987	0.985	0.985	0.970	0.980	0.993	0.980	0.985	0.990	0.992	0.992	0.992	SAGEM MD Coating	
Collimating Triplet Total	0.970	0.974	0.970	0.972	0.967	0.972	0.969	0.969	0.967	0.969	0.970	0.970	0.970	0.970	0.969	0.965	0.965	0.966	0.968		
Reflection Losses (2 surfaces)	0.986	0.980	0.974	0.976	0.970	0.976	0.972	0.972	0.970	0.972	0.974	0.974	0.974	0.974	0.972	0.969	0.970	0.972	0.976	Master AR Coating	
Lens 1	0.995	0.998	0.998	0.998	0.998	0.998	0.998	0.998	0.998	0.998	0.998	0.998	0.998	0.998	0.998	0.998	0.997	0.996	0.995	S-FSL5V (22.97 mm)	
Lens 2	1.000	1.000	1.000	1.000	1.000	1.000	1.000	1.000	1.000	1.000	1.000	1.000	1.000	1.000	1.000	1.000	1.000	1.000	1.000	COPCAF2 (33.18 mm)	
Lens 3	0.989	0.996	0.998	0.998	0.998	0.998	0.998	0.998	0.998	0.998	0.998	0.998	0.998	0.998	0.998	0.998	0.997	0.997	0.996	PBL6Y (18.71 mm)	
ADC Prism 1	0.970	0.974	0.970	0.972	0.967	0.972	0.969	0.969	0.967	0.969	0.970	0.970	0.970	0.970	0.969	0.965	0.965	0.965	0.968		
Reflection Losses (2 surfaces)	0.986	0.980	0.974	0.976	0.970	0.976	0.972	0.972	0.970	0.972	0.974	0.974	0.974	0.974	0.972	0.969	0.970	0.972	0.976	Master AR Coating	
ADC 1A	0.996	0.998	0.998	0.998	0.998	0.998	0.998	0.998	0.998	0.998	0.998	0.998	0.998	0.998	0.998	0.998	0.997	0.996	0.996	S-FSL5V (20.00 mm)	
ADC 1B	0.988	0.996	0.998	0.998	0.998	0.998	0.998	0.998	0.998	0.998	0.998	0.998	0.998	0.998	0.998	0.998	0.997	0.996	0.996	PBL6Y (20.00 mm)	
ADC Prism 2	0.970	0.974	0.970	0.972	0.967	0.972	0.969	0.969	0.967	0.969	0.970	0.970	0.970	0.970	0.969	0.965	0.965	0.965	0.968		
Reflection Losses (2 surfaces)	0.986	0.980	0.974	0.976	0.970	0.976	0.972	0.972	0.970	0.972	0.974	0.974	0.974	0.974	0.972	0.969	0.970	0.972	0.976	Master AR Coating	
ADC 2A	0.988	0.996	0.998	0.998	0.998	0.998	0.998	0.998	0.998	0.998	0.998	0.998	0.998	0.998	0.998	0.998	0.997	0.996	0.996	PBL6Y (20.00 mm)	
ADC 2B	0.996	0.998	0.998	0.998	0.998	0.998	0.998	0.998	0.998	0.998	0.998	0.998	0.998	0.998	0.998	0.998	0.997	0.996	0.996	S-FSL5V (20.00 mm)	
Focusing Triplet Total	0.970	0.974	0.970	0.972	0.967	0.972	0.969	0.969	0.967	0.969	0.970	0.970	0.970	0.970	0.969	0.965	0.965	0.966	0.968		
Reflection Losses (2 surfaces)	0.986	0.980	0.974	0.976	0.970	0.976	0.972	0.972	0.970	0.972	0.974	0.974	0.974	0.974	0.972	0.969	0.970	0.972	0.976	Master AR Coating	
Lens 1	0.989	0.996	0.998	0.998	0.998	0.998	0.998	0.998	0.998	0.998	0.998	0.998	0.998	0.998	0.998	0.998	0.997	0.997	0.996	PBL6Y (18.71 mm)	
Lens 2	1.000	1.000	1.000	1.000	1.000	1.000	1.000	1.000	1.000	1.000	1.000	1.000	1.000	1.000	1.000	1.000	1.000	1.000	1.000	COPCAF2 (33.18 mm)	
Lens 3	0.995	0.998	0.998	0.998	0.998	0.998	0.998	0.998	0.998	0.998	0.998	0.998	0.998	0.998	0.998	0.998	0.997	0.996	0.995	S-FSL5V (22.97 mm)	

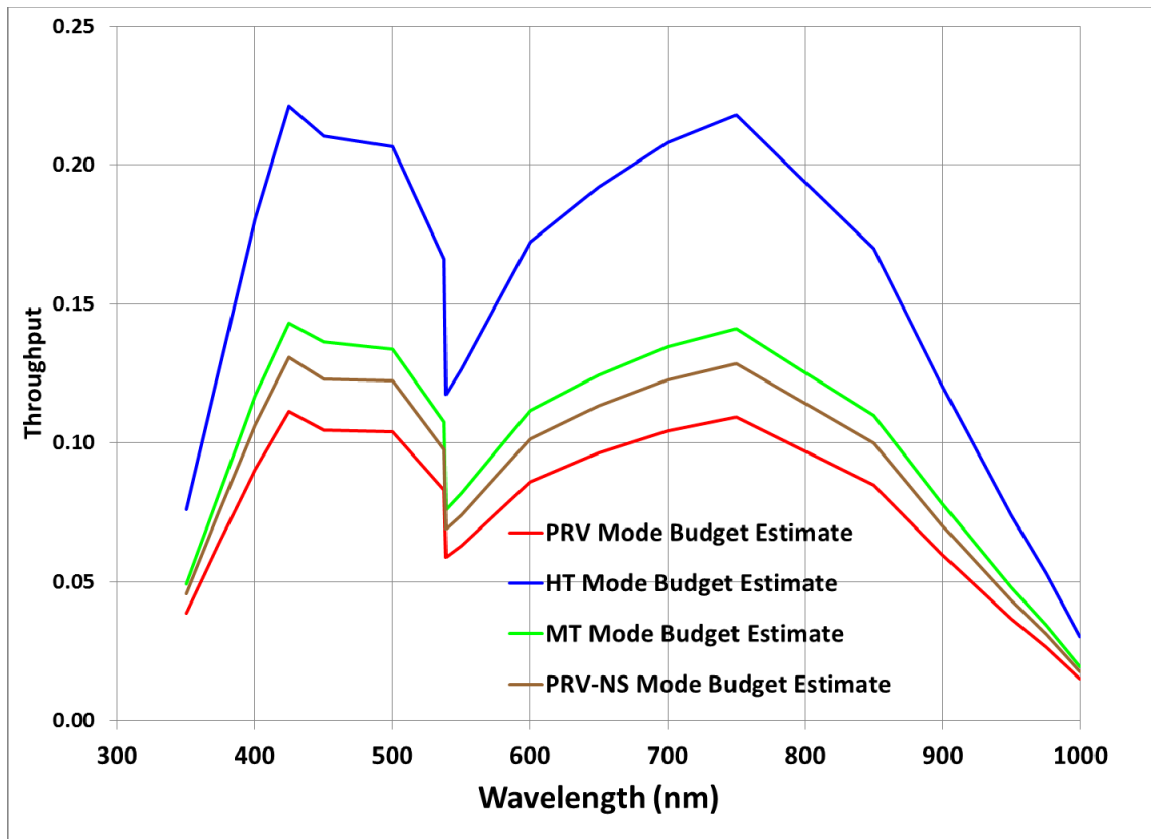


Figure 8. Estimates of Throughput for G-CLEF Observing Modes

5. IMPACT OF ADAPTIVE OPTICS (AO)

G-CLEF will be designed to take advantage of the GMT adaptive optics (AO) capabilities when they become available. The GMT natural guidestar ground layer AO (NG GLAO) mode will be implemented using wavefront sensors external to G-CLEF. Implementation of the natural guidestar AO (NGAO) mode will require the addition of an NGAO wavefront sensor into the G-CLEF front end. The interface for this sensor is being designed into G-CLEF. These AO modes, when implemented at the GMT, will enhance the PRV measurement capability and the throughput of G-CLEF. AO will improve the telescope image quality and stability over the natural seeing image quality. For example, the FWHM in NG GLAO mode is under $0.5''$ ($.5 \mu\text{m}$ to $1 \mu\text{m}$ band) and the RMS image motion is reduced to less than 40 mas, vs. 68 mas for natural seeing. This improvement in telescope image quality and stability has positive impacts on G-CLEF performance. A sharper image improves the throughput significantly as it reduces slit losses. The stability of the telescope image directly reduces the external, non-calibratable error term in the PRV budget. We expect that these improvements, combined with better calibration sources, will enable G-CLEF to meet the PRV goals and generally enhance G-CLEF scientific performance.

6. CONCLUSIONS

The G-CLEF instrument is being designed and built using current systems engineering best practice. Requirements definition, flow down, verification and error budgeting are integral parts of the process. This approach is in conformance with the GMT requirements and is consistent with the approach being utilized to design and build the GMT itself. This approach is necessary, given the scale of investment in the GMT and its instruments, and will help ensure that the science objectives will be met.

Examples of error budgets have been presented. The PRV budget is particularly challenging because many of the components are not amenable to analysis, and there is a complex interaction between measurement and calibration. Even so, the PRV budget presented is a useful tool and provides a road map towards meeting the PRV measurement requirements. The throughput budget is an example of a straight-forward budgeting tool, similar to that used in many other programs, which helps the program manage one of its key requirements.

REFERENCES

- [1] Johns, M., McCarthy, P., Raybould, K., Bouchez, A., Farahani, A., Filgueira, J., Jacoby, G., Sheckman, S., Sheehan, M., "Giant Magellan Telescope – Overview", SPIE 8444-52, 2012
- [2] Szentgyorgyi, A., et. al., "A Preliminary Design for the GMT-Consortium Large Earth Finder (G-CLEF)," SPIE 9147-78, 2014
- [3] Furesz, G., et. al., "The G-CLEF spectrograph optical design – and update to the venerable white pupil echelle configuration," SPIE 9147-353, 2014
- [4] Mueller, M., et. al., "The Opto-Mechanical Design of the GMT-Consortium Large Earth Finder (G-CLEF)," SPIE 9147-347, 2014
- [5] Lovis, C. and Pepe, F., "A new list of thorium and argon spectral lines in the visible," *Astronomy & Astrophysics*, February 5, 2008.
- [6] Li, C. et. al., "Green astro-comb for HARPS-N", SPIE 8446-8XL
- [7] Phillips, D. F., et. al., "Calibration of an echelle spectrograph with an astro-comb: a laser frequency comb with very high repetition rate", SPIE 8446-8OP
- [8] Edlén, B., "The refractive index of air," *Metrologia* 2, 71-80 (1966).
- [9] Hrudkov'a, M., "The Accurate Barycentric Corrections for the Detection of Extrasolar Planets," WDS'06 Proceedings of Contributed Papers, Part III, 18–23, 2006
- [10] Furesz, g., et. al., "Practical aspects of building fiber links for precision radial velocity instruments", SPIE 9151-73, 2014
- [11] Chazelas, B., Pepe, F. and Wildia, F., "Optical fibers for precise radial velocities: an update", SPIE 8450-13, 2012
- [12] Szentgyorgyi, A., "Notes on Modeling Seeing at Las Campanas," GC-131111.b, Nov. 11, 2013